

# Optimal control towards sustainable wastewater treatment plants based on deep reinforcement learning

Kehua Chen<sup>1,a,d</sup>, Hongcheng Wang<sup>1,a,b</sup>, Borja Valverde Pérez<sup>c</sup>, Luca Vezzaro<sup>c,\*,</sup>, Aijie Wang<sup>a,\*</sup>

<sup>a</sup>*Key Lab of Environmental Biotechnology, Research Center for Eco-Environmental Sciences, Chinese Academy of Sciences, 18 Shuangqing Road, Haidian District, Beijing, 100085, China*

<sup>b</sup>*School of Civil & Environmental Engineering, Harbin Institute of Technology (Shenzhen), Shenzhen 518055, PR China*

<sup>c</sup>*DTU Environment, Technical University of Denmark, Bygningstorvet, Building 115, 2800 Kongens Lyngby, Denmark*

<sup>d</sup>*Sino-Danish Center for Education and Research, University of Chinese Academy of Sciences, Beijing, China*

---

## Abstract

Wastewater treatment plants (WWTPs) are designed to eliminate pollutants and alleviate environmental pollution resulting from human activities. However, the construction and operation of WWTPs still have negative impacts. WWTPs are complex to control and optimize because of high non-linearity and variation. This study used a novel technique, multi-agent deep reinforcement learning (MADRL), to optimize dissolved oxygen (DO) and chemical dosage in a WWTP. The reward function is specially designed as life cycle assessment (LCA)-based form to achieve sustainability optimization. Five scenarios are considered: baseline, LCA-oriented Class I-A, LCA-oriented Class I-B, cost-oriented and LCA-oriented Surface Water IV. The result shows that optimization based on LCA has lower environmental impacts compared to baseline scenario. The cost-oriented control strategy owns comparable performance to the LCA-driven strategy, but with less extendability. It is worth mentioning that the retrofitting of WWTPs based on resources should be implemented with the consideration of impact transfer. The major contributors of each indicators are identified for future study and improvement. Last, we discuss that novel dynamic control strategies require advanced sensors or a large amount of data, so the selection of control strategies should also consider economic and ecological conditions. In a nutshell, there are still limits and shortcomings of this work and future studies are required.

*Keywords:* Wastewater treatment, reinforcement learning, multi-objective optimization, sustainability

---

## 1. Introduction

### 1.1. Motivation

With an increasing population and the acceleration of urbanization and industrialization, a large amount of wastewater is being produced. Wastewater treatment plants (WWTPs) have been designed to eliminate contaminants and alleviate environmental pollution of wastewater resulting from human activities. Normally, there are four phases in treating wastewater: pre-treatment, primary treatment, secondary treatment, and tertiary treatment, and each phase has plenty of technologies to choose from. From a global scale, WWTPs have positive effects in environment protection (Rosso and Stenstrom, 2008). However, the construction and operation of WWTPs consume resources (freshwater, energy, chemicals, etc.), emit greenhouse gases (GHGs) and produce residual sludge. WWTPs are complex to control and optimize because of high non-linearity and variation. At present, traditional control strategies driven by Single Objective Optimization (SOO) are lack of systematic thinking (Yang et al., 2014). At present, the main focus of WWTPs lies on energy consumption, ignoring a comprehensive evaluation of the impact caused by WWTPs. For example, set-points of aeration rate are normally determined by nitrogen and BOD removal efficiency (Åmand et al., 2013). Nevertheless, the content of dissolved oxygen (DO) can also affect the emission of nitrous oxide ( $N_2O$ ) (Castro-Barros et al., 2015) and chemical dosage. With the rise of environmental consciousness, the optimization towards sustainability is imperative.

### 1.2. Related work and contributions

Model Predictive Control (MPC) utilizes an explicit model to predict future responses of a system. In wastewater treatment, Holenda et al. (2008) applied MPC technique to

---

\*ajwang@rcees.ac.cn

\*\*luve@env.dtu.dk

1.Kehua Chen and Hongcheng Wang contributed equally to this article

control DO in an activated sludge process; Nonlinear MPC (NMPC) was applied in ASM2d model to achieve optimal control (Grochowski and Rutkowski, 2016). Although MPC is a power method to control dynamic systems, MPC requires detailed models, and controlling nonlinear systems such as WWTPs consume high computational time. Therefore, data-driven or model-free algorithms try to handle these drawbacks.

Since the release of Alpha GO (Silver et al., 2016), Reinforcement Learning (RL) has received much attention to optimize different processes in WWTPs. RL is a branch of machine learning, where an agent learns from interacting with the environment (Kaelbling et al., 1996). Hernández-del Olmo et al. (2012) applied value-based RL in WWTP to minimize effluent ammonia and energy consumption simultaneously. The environment was modelled based on Benchmark Simulation Model No.1 (BSM1). In order to communicate accurately, operation cost was used as the metric. Syafie et al. (2011) used Q-learning (Watkins and Dayan, 1992) to control oxidation process in WWTP according to oxidation-reduction potential measurement. Temporal abstraction was applied to reduce the amount of non-relevant exploration and the calculation time. The aim of the agent was to maintain oxidation-reduction potential (ORP) at specific point. The ORP level was discrete based on measurement noise. Furthermore, the hydraulic retention time (HRT) of anaerobic and aerobic reactors was optimized by Q-learning in activated sludge process based on ASM2d model (Pang et al., 2019a,b). The state was generated according to effluent COD and TP, and the agent updated the HRT under four different step-lengths. However, Q-learning is under tabular formulation and can only handle discrete state and action spaces. Different from value-based algorithms, policy-based algorithms naturally represent state and action spaces continuously. REINFORCE algorithm was used to control bioprocesses (Pet-sagkourakis et al., 2020). The control policy was parameterized by recurrent neural network. The agent was firstly trained off-line in a simulated environment, after transfer learning, the algorithm was applied on the true system. A novel policy-based algorithm, proximal policy optimization (PPO), was applied to optimize the control of pump station in WWTPs (Filipe et al., 2019). The actions were sampled from Beta distribution. Tank level and pump consumption were integrated as the reward function, therefore, the aim of the agent was to

control tank level within reasonable range and reduce energy consumption.

As a cradle-to-grave or cradle-to-cradle analysis technique, numerical Life Cycle Assessment (LCA) has been integrated into mathematical optimization as objective functions. [de Faria et al. \(2016\)](#), [Li et al. \(2018\)](#) and [Ahmadi and Tiruta-Barna \(2015\)](#) used LCA model to solve Multi-Objective Optimization (MOO) problems, thus achieving minimization of environmental impacts, which provided more comprehensive guidance on management and design of water facilities. Nevertheless, the research of optimal control based on LCA is still at the initial stage.

### 1.3. Paper overview

This paper focuses on real-time optimal control in an activated sludge based WWTP. An actor-critic algorithm with multi-agents, Multi-Agent Deep Deterministic Policy Gradient (MADDPG), is applied to achieve the control of dissolved oxygen and chemical dosage in a WWTP under continuous action and state spaces. In order to obtain sustainable control strategies, various reward functions are adopted and compared. The structure of this paper is as follows: in Section 2, the layout of the WWTP and problem formulation are introduced, leading to the description of the learning process. In Section 3, different scenarios are compared and discussed, limitation and future work are introduced.

## 2. Methodology

### 2.1. WWTP overview

A WWTP based on activated sludge is optimized in this study as Fig. 1 shows. The main process includes primary sedimentation, biological treatment, secondary sedimentation, filtration and sludge treatment. The sludge is treated by thickening, chemical dosing, digestion and dewatering. The WWTP is located in Jiangsu Province, China, with a population equivalent around 10,000. The volumes of primary clarifier, anaerobic tank, anoxic tank 1, anoxic tank 2, aerobic tank and secondary clarifier are 300, 200, 400, 600, 800 and 600  $m^3$  respectively. The sludge recycling ratio is set as 150%, and the internal recycling ratio (IRR) between anoxic tank 1 and anaerobic tank is 300%, the IRR between aerobic

tank 2 and anoxic tank 2 is 200%. To further eliminate phosphorus, chemical precipitation is implemented in aerobic tank with 25% Polyaluminium Chloride (PAC) solution. For sludge treatment, 40% ferric chloride solution is applied for sludge pre-treatment before digestion. Water from thickening and dewatering returns back to primary clarifier. The treated sludge is transported for land-filling. The WWTP is simulated with MANTIS model developed by Hydromantis GPS-X. As a comprehensive model, MANTIS model integrated ASM2d, UCTADM1 (Sötemann et al., 2005) and Musvoto precipitation model (Van Rensburg et al., 2003).

The characteristics of influents are shown in Table S1. Dynamic influent data are generated based on literature (Gernaey et al., 2011; Flores-Alsina et al., 2012). Since the SRT is 15 days, the first 20-day simulation is used to reach steady state, while the following 10 days are used for optimization.

Under baseline scenario, DO and chemical dosage are constant with a closed-loop control. Specifically, the DO set-point is 1.5 mg/L, and the phosphorus precipitation dosage is 0.125  $kg/m^3\text{-}ww$ . The system boundary of LCA is confined within the WWTP.

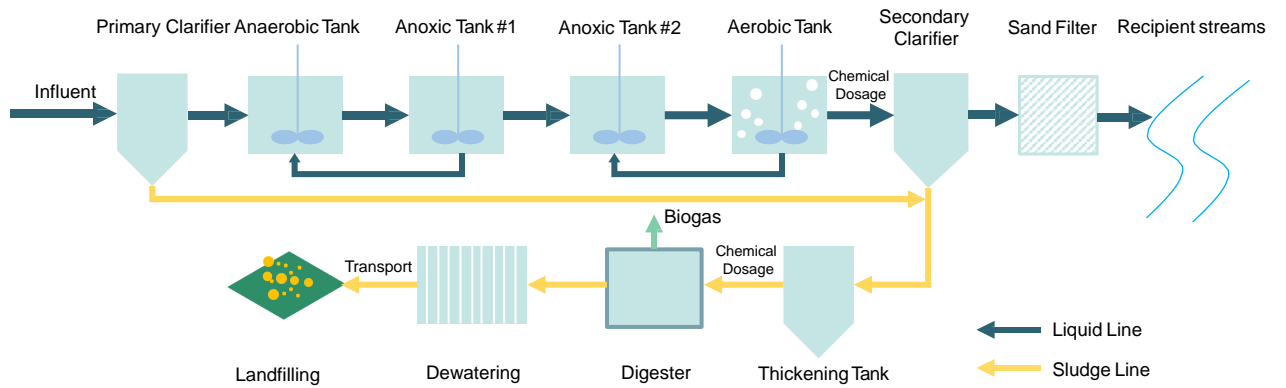


Figure 1: WWTP layout

## 2.2. Problem Statement

In this study, a popular actor-critic algorithm in RL, DDPG, is used (Lillicrap et al., 2015) as shown in Fig.2. Considering a standard RL problem, we model the environment  $E$

as Markov decision process with state space  $\mathcal{S}$ , action space  $\mathcal{A}$ , an initial state distribution  $p(s_1)$ , transition dynamics  $p(s_{t+1}|s_t, a_t)$ , and reward function  $r(s_t, a_t)$ . An agent interacts with the environment by choosing different actions  $a_t \in \mathbb{R}^N$  at timestep  $t$ . After each interaction, the environment releases state  $s_t$ . Agent's behaviors are defined by a stochastic policy,  $\pi$ , which maps states to actions ( $\pi : \mathcal{S} \rightarrow \mathcal{P}(\mathcal{A})$ ). When the environment is not fully observable, state space is replaced by observation space  $\mathcal{O}$ .

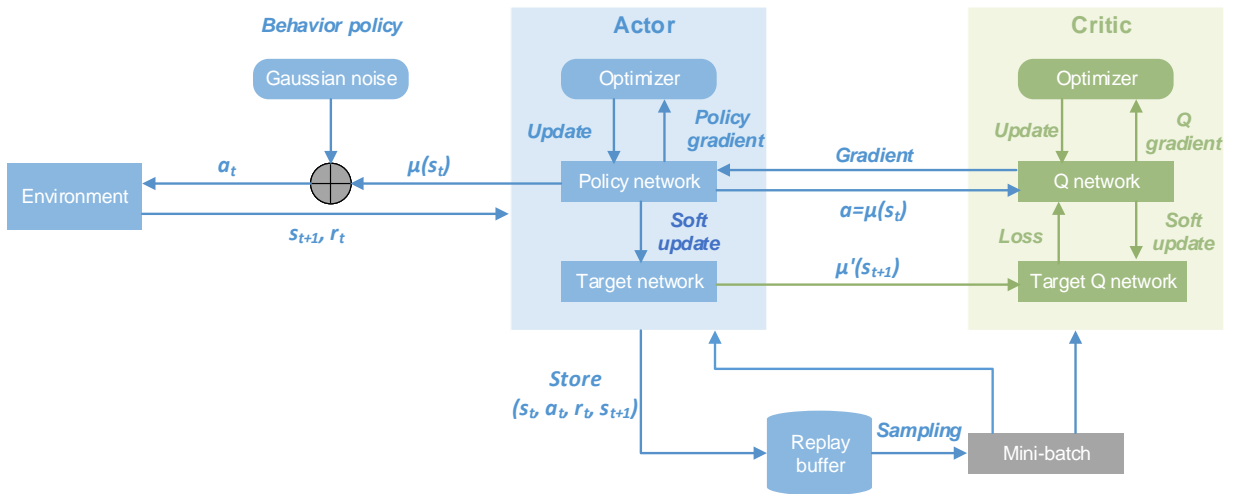


Figure 2: DDPG algorithm structure

The return is defined as the sum of discounted future reward:

$$R_t = \sum_{i=t}^T \gamma^{(i-t)} r(s_i, a_i) \quad (1)$$

in which  $\gamma \in [0, 1]$  is the discount factor.

The aim of RL is to find an optimal policy that maximizes expected return:

$$\max_{\pi(\cdot)} \mathbb{E}_{r_i, s_i \sim E, a_i \sim \pi} [R_t | s_t, a_t] \quad (2)$$

Many RL algorithms acquire expected return by calculating action-value functions recursively, e.g. Bellman equation:

$$Q^\pi(s_t, a_t) = \mathbb{E}_{r_t, s_{t+1} \sim E}[r(s_t, a_t) + \gamma \mathbb{E}_{a_t \sim \pi}[Q^\pi(s_{t+1}, a_{t+1})]] \quad (3)$$

In DDPG, a parameterized deterministic policy  $\mu(s|\theta^\mu)$  is considered with parameter  $\theta^\mu$ . The critic  $Q(s, a)$  is learned using the Bellman equation, while the actor is updated by the gradient of expected return from initial state with respect to actor parameters  $\theta^Q$ :

$$\nabla J_{\theta^\mu} \approx \mathbb{E}_{s_t}[\nabla_{\theta^\mu} Q(s, a|\theta^Q)_{s=s_t, a=\mu(s_t|\theta^\mu)}] \quad (4)$$

$$= \mathbb{E}_{s_t}[\nabla_a Q(s, a|\theta^Q)_{s=s_t, a=\mu(s_t)} \nabla_{\theta^\mu}(s|\theta^\mu)_{s=s_t}] \quad (5)$$

Similar to Deep Q-Network (Mnih et al., 2015), a replay buffer  $\mathcal{R}$  is used in DDPG. Transitions are sampled from the environment by an exploration policy, and the tuple  $(s_t, a_t, r_t, s_{t+1})$  are stored in the replay buffer. Gaussian noise is used for exploration. When the replay buffer is full, oldest experiences are discarded. Furthermore, soft target updates are applied in order to avoid divergence of Q update. Target networks are firstly copied from actor and critic networks, i.e.  $\mu'(s_t|\theta^{\mu'})$  and  $Q'(s_t, a_t|\theta^{Q'})$ . Then these target networks update slowly with learned networks:

$$\theta' \leftarrow \tau\theta + (1 - \tau)\theta' \quad (6)$$

in which,  $\tau \ll 1$ .

In this study, two agents are deployed in terms of multi-agent paradigm, i.e. MADDPG (Lowe et al., 2017). In detail, one agent is for DO control and the other is for dosage control. Normally, multi-agent algorithms have decentralized actor and centralized critic, which means each actor receives its own observations and outputs single actions but critic network of each agent receives complete observations (Fig. 3).

In this paper, the optimization problem is abstracted to a sequential decision problem. The environment is the WWTP model as described in Section 2.1 coupled with interaction interface, and the agents try to set dissolved oxygen (DO) and chemical dosage in terms

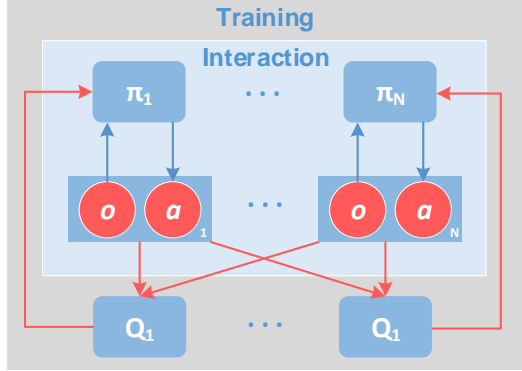


Figure 3: Overview of multi-agent structure

of deterministic policies. The observation of agents includes: (i) influent COD, TN, TP and  $\text{NH}_3\text{-N}$ ; (ii) inflow rate; (iii) time; (iv) current DO and dosage respectively. After each interaction, a reward signal is released by the environment. The reward function is designed based on cost and LCA (see Section 2.4). The aim of the agents is to minimize negative impacts of the studied WWTP.

### 2.3. Learning process

The MADDPG learning process mainly follows the original paper (Lowe et al., 2017) and is introduced in this section. Different from the original paper, Gaussian noise  $\mathcal{N}$  rather than Ornstein-Uhlenbeck process is used for exploration. Hyperparameters of MADDPG are fine tuned and listed in Table S2. Before training, 10,000 sample data are acquired by Monte Carlo sampling from uniform distribution. The value of DO ranges from 0 to 5  $mg/L$ , and chemical dosage ranges from 0 to 0.5  $kg/m^3\text{-}ww$ .

**Step 0, Initialization:** Randomly initialize actor and critic weights  $\theta_i^\mu$  and  $\theta_i^Q$  for  $i$ -th agent. Initialize target networks as  $\theta_i^{\mu'} = \theta_i^\mu$ ,  $\theta_i^{Q'} = \theta_i^Q$ . Initialize replay buffer  $\mathcal{R}$ . Calculate the rewards of the sample points, obtain maximum and minimum values of each term for normalization. The initial state  $o$  is randomly chosen from the sample points.

**Step 1, Interaction:** The behavior policy  $\beta_i$  receives the observation vector and outputs action  $a_i$  to the environment.

$$a_{t,i} = \mu(o_{t,i} | \theta^\mu) + \mathcal{N}_t \quad (7)$$

The environment then interacts with GPS-X model and the agent receives a new observation  $o'$ . Reward  $r_{t,i}$  is then calculated based on the new state, tuple  $(o, a_{t,i}, r_{t,i}, o')$  is stored in the replay buffer  $\mathcal{R}$ . If the replay buffer is full, oldest samples will be discarded.

**Step 2, Network training:** Randomly sample  $N$  transitions ( $N=256$  in this study) in the replay buffer as a mini-batch. For critic network, loss  $L$  is calculated by mean squared loss (MSE). The critic gradient is thus  $\nabla_{\theta_i^Q} L$ .

$$L_i = \frac{1}{N} \sum_j (y^j - Q_i^\mu(o^j, a_1^j, \dots, a_N^j | \theta_i^Q))^2 \quad (8)$$

$$y^j = r_i^j + \gamma Q_i^{\mu'}(o'^{j+1}, a_1'^j, \dots, a_N'^j) \Big|_{a_k' = \mu'_k(o_k^j)} \quad (9)$$

Actor gradient is obtained from the deterministic policy gradient derived from [Silver et al. \(2014\)](#).

$$\nabla_{\theta_i^\mu} J \approx \frac{1}{N} \sum_j \nabla_{a_i} Q_i^\mu(o^j, a_1^j, \dots, a_N^j) \Big|_{a_k = \mu_k(o^j)} \nabla_{\theta_i} \mu_i(o^j) \quad (10)$$

Each agent  $i$  updates parameters in terms of equation 8 - 10. Policy networks are updated by Adam optimizer ([Kingma and Ba, 2014](#)), target networks are updated using soft updating method. After each epoch, the noise will decay 0.003%.

**Step 3, Repetition:** If time-step reaches  $T = 6000$ , stop; otherwise back to Step 1.

The algorithm is coded with Pytorch version 1.5 ([Ketkar, 2017](#)) under Python 3.7 environment. The environment is achieved with the RL toolkit, Gym, developed by OpenAI ([Brockman et al., 2016](#)).

#### 2.4. Reward function

Life cycle cost and several LCA mid-point indicators are chosen to form the reward function. Normalization is then applied to ensure a balanced evaluation. For each dynamic

simulation, mean values within 10 days are recorded to calculate rewards. Since the DO and dosage mainly affect biological process and sludge production, other environmental impacts are considered as constant hence are ignored in the optimization problem.

#### 2.4.1. Cost

The total operational cost is divided into five components: energy cost, transportation cost, chemicals cost, sludge disposal cost and biogas benefits. The prices are acquired from market investigation ([Alibaba, 2020](#)) and literatures.

- (1) Energy cost  $C_e$ : unit price of electricity is 0.8 CNY/kWh, and consumption is derived from Section [2.4.2](#), only direct energy consumption is considered.
- (2) Transportation cost  $C_t$ : unit price is 0.6 CNY/kg, the cost encompasses transportation of chemicals and treated sludge.
- (3) Chemical cost  $C_c$ : ferric chloride solution (40%) is assumed to pre-treat sludge, with a price of 1.7 CNY/kg for  $FeCl_3$ (100%); 25% PAC solution is applied for phosphorus removal, with a price of 2.5 CNY/kg for PAC (100%).
- (4) Sludge landfill cost  $C_s$ : residual sludge is transported for landfilling, and the treatment cost is 0.52 CNY/kg ([Yang et al., 2015](#)).
- (5) Biogas price: biogas is generated from digester and the subsidy of renewable energy is 0.25 CNY/kWh ([Jiang et al., 2011](#)). The specific model is demonstrated in [Supplementary Information](#).

The total cost is the sum of five parts:

$$C_{tot} = C_e + C_t + C_c + C_s - C_{bio} \quad (11)$$

where  $C_{tot}$  is total cost in unit CNY/ $m^3$ -*ww* ( $m^3$ -wastewater).

#### 2.4.2. LCA mid-point indicators

**Energy Consumption.** Since aeration rate and dosage are the main factors are optimized and controlled in this study, energy consumed by aeration and sludge treatment processes

are included in reward function. Energy consumed by mixing, heating or other pumping processes is assumed as constant, thus is ignored. Specifically, three components are consisted of energy consumption.

- (1) Dissolved oxygen is controlled by aeration mechanical power, with a fixed set-point, aeration power  $p_a$  is controlled in terms of influent quality by a Proportional-Integral (PI) controller.
- (2) Energy consumption of pumps includes residual sludge pump, thickening pump, dewatering pump. The energy consumption is calculated by equation 12 and 13.

$$H = H_{static} + H_{dynamic} \quad (12)$$

$$W = \frac{\rho g Q H}{1000 \eta} \quad (13)$$

where  $W$  is the pump power, kWh;  $\rho$  is water density,  $1000 \text{ kg/m}^3$ ;  $g$  is acceleration of gravity,  $9.8 \text{ m/s}^2$ ;  $Q$  is flow rate,  $\text{m}^3/\text{s}$ ;  $H$  is pumping head,  $\text{m}$ ;  $\eta$  is pump efficiency, 0.7. The static water head  $H_{static}$  is set as 5 m, and the frictional head loss is assumed as constant, 1 m.

- (3) WWTPs often use chemicals to remove pollutants or pre-treat sludge. Chemicals also consume energy during production and transportation. According to [Longo et al. \(2019\)](#), energy consumption related to iron chloride (40%) and PAC (25%) is 3.4 and 1.94 kWh/kg respectively.

In a nutshell, total energy consumption is:

$$E_{tot} = E_{aer} + E_{tran} + E_{che} \quad (14)$$

where  $E_{tot}$  is total cost in unit  $\text{kWh/m}^3\text{-ww}$ .

**Eutrophication potential.** Eutrophication potential measures underlying nutrient discharge of the system to recipient streams by emission factors, in unit  $\text{kg PO}_4\text{-eq}$ . Emission factors from CML database ([CML, 2002](#)) are shown in Table 1:

Table 1:  $PO_4$  emission factors of various substances

Item	Emission factor ( $kgPO_4\text{-eq}/kg$ )
$TP$	3.07
$COD$	0.022
$NH_4^+$	0.33
$NO_3^-$	0.095
$NO_2^-$	0.13

Thus, eutrophication potential can be derived as:

$$EP = 3.07 \cdot TP_{eff} + 0.022 \cdot COD_{eff} + 0.33 \cdot NH_4_{eff}^+ + 0.095 \cdot NO_3_{eff}^- + 0.13 \cdot NO_2_{eff}^- \quad (15)$$

where  $EP$  is total value in unit  $kgPO_4\text{-eq}/m^3\text{-ww}$ ;  $TP_{eff}$ ,  $COD_{eff}$ ,  $NH_4_{eff}^+$ ,  $NO_3_{eff}^-$ ,  $NO_2_{eff}^-$  represent effluent TP, COD,  $NH_4^+$ ,  $NO_3^-$  and  $NO_2^-$  respectively.

**Greenhouse gas emission.** There are three scopes in GHG emissions: process emissions, energy emissions and material emissions. Process emissions are complicated. MANTIS model in GPS-X encompasses greenhouse gas module and simulates the emission of  $N_2O$  and  $CH_4$  (Goel et al., 2012). In detail,  $N_2O$  and  $CH_4$  emitted by anaerobic tank, anoxic tank, aerobic tank and digester are considered, emissions from clarifiers and other sludge treatment processes are ignored in the model. In addition, nitrous oxide and methane emission from effluent are estimated using emission factors from IPCC (Eggleston et al., 2006).

$$CH_{4eff} = BOD_{eff} \cdot B_o \cdot MCF \quad (16)$$

$$N_2O_{eff} = TN_{eff} \cdot EF \cdot \frac{44}{28} \quad (17)$$

in which,  $CH_{4eff}$  is methane emission rate,  $kgCH_4/d$ ;  $BOD_{eff}$  is effluent BOD concentrate,  $kgBOD/d$ ;  $B_o$  is maximum  $CH_4$  producing capacity,  $0.25\ kgCH_4/kgBOD$ ;  $MCF$  is methane correction factor, 0.035 (fraction);  $N_2O_{eff}$  is nitrous oxide emission rate,  $kgN_2O/d$ ;  $TN_{eff}$  is nitrogen in the effluent discharged to aquatic environments,  $kgN/d$ ;  $EF$  is emission factor for  $N_2O$  emissions from wastewater discharged to aquatic systems,  $0.016\ kgN_2O-N/kgN$ ; the factor 44/28 is the conversion factor of  $kgN_2O-N$  into  $kgN_2O$ .

Indirect emissions associated to energy consumption can be calculated according to a factor based on the energy mix for China (Wang et al., 2016). Emissions are derived based on various emission factors Table 2.

Table 2: GHG Emission factors

Item	Emission factor	Reference
<i>Electricity</i>	$1.17\ kgCO_2-eq/kWh$	(Wang et al., 2016)
<i>FeCl<sub>3</sub>(100%)</i>	$0.986\ kgCO_2-eq/kg\ FeCl_3$	(Parraviciniak et al., 2016)
<i>PAC(100%)</i>	$1.182\ kgCO_2-eq/kgPAC$	(de Haas et al., 2008)
<i>Transportation(road)</i>	$0.000192\ kgCO_2-eq/(kg \cdot km)$	(Zhang and Wang, 2016)
<i>Nitrous oxide</i>	$298\ kgCO_2-eq/kg\ N_2O$	(Egginton et al., 2006)
<i>Methane</i>	$25\ kgCO_2-eq/kg\ CH_4\ N_2O$	(Egginton et al., 2006)

Here, we assume that all chemicals and sludge are transported through road, with average distance as 200 km. The equation for global GHG estimation is:

$$GHG_{tot} = GHG_{pro} + GHG_{energy} + GHG_{material} \quad (18)$$

where  $GHG_{tot}$  is total value in unit  $kgCO_2-eq/m^3-ww$ .

**Weighted sum.** For LCA scenario, the reward function is derived by combining energy consumption, eutrophication potential and greenhouse gas emission. Normalization is required for the comparison of different indicators, hence we need maximum and minimum

values in advance. Here, maximum and minimum values are obtained by sampling: sampling data from uniform distribution before training, i.e. internal normalization (Pizzol et al., 2017).

$$Item_{norm} = \frac{Item_{tot} - Item_{min}}{Item_{max} - Item_{min}}, \quad (19)$$

$$\forall Item \in I = \{E, EP, GHG\}.$$

Therefore, the reward function is as follows:

$$Reward = w_E E_{norm} + w_{EP} EP_{norm} + w_{GHG} GHG_{norm} \quad (20)$$

where  $w_E$ ,  $w_{EP}$  and  $w_{GHG}$  indicate weights of energy consumption, eutrophication potential and greenhous gas emission, respectively.

Wang et al. (2015) applied a data-driven method and found that weights differ in mid-point indicators. However, his study shows that struvite capture (indicating the influence of nutrients), energy consumption and GHG emissions in developing countries actually have similar contributions. Although there are some differences of components in each indicator between Wang's study and our study, three parts are treated equally in this study, i.e. each weight is 0.33.

#### 2.4.3. Extra constraints

In order to obtain reasonable results, an extra constraint is added in the reward function. The constraint is effluent quality with specific limits. If the effluent concentrations exceed the thresholds, an extra penalty +1 will be added to the total reward.

At last, the reward is multiplied by -1 to keep consistency with the maximization setting.

#### 2.5. Scenario introduction

Nowadays, the stakeholders generally optimize control strategies based on cost under the constraint of discharge standards. Recently, the Chinese government proposed the Action Plan for Water Pollution Prevention and Control (Ministry, 2014), which requires all

WWTPs in protected areas to meet the Grade I-A standard of effluent discharge. In some specific areas, the standards are even stricter than Grade I-A (Zhang et al., 2016), i.e. the quasi standard IV for surface water. Common standards are listed in Table S3, and the quasi standard IV for surface water only covers TP, TN, COD and ammonia. Therefore, environmental impacts of five scenarios are compared to present the results with different emphasis:

- (1) Baseline scenario, parameters are determined according to the experience, here, DO is set as 1.5 mg/L and dosage is  $0.125 \text{ kg/m}^3\text{-ww}$ .
- (2) Global sustainability scenario I-A (LCA-IA), optimization based on LCA is implemented under Class I-A standard.
- (3) Cost scenario, optimization based on cost is implemented under Class I-A standard.
- (4) Global sustainability scenario I-B (LCA-IB), optimization based on LCA is implemented under Class I-B standard.
- (5) Global sustainability scenario quasi standard IV for surface water (LCA-SW), optimization based on LCA is implemented under quasi surface water IV standard.

### 3. Results and discussion

#### 3.1. Training results

Fig. 4 shows the reward vary with training steps under LCA scenario. The shadow in the figure shows the standard deviation among five paralleled experiments. At the beginning, the reward is low and has high variance since the initialization of weights is random and the policies have high noise to explore the action space. At the end stage, the agents learn the optimal policies and exploit the historical information sufficiently. However, since multiple value combinations lead to the similar performance, the variance still exists. In the test or deployment phase, the exploration noise changes to zero.

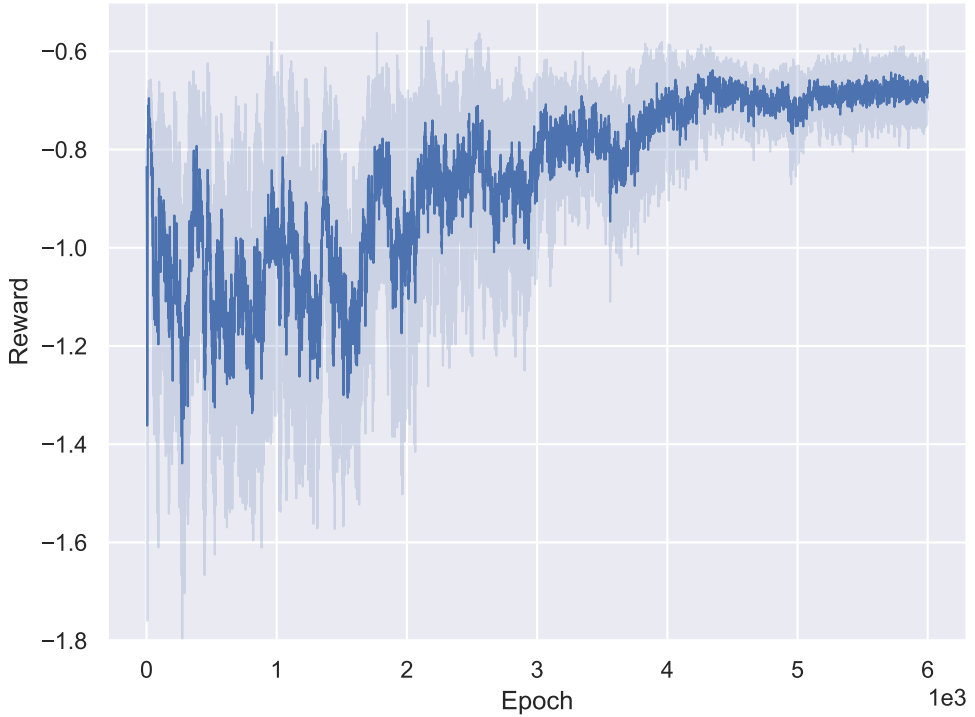


Figure 4: Reward variation under LCA scenario, the shadow is the standard deviation of 5 experiments.

The representations learned by critic networks are examined by using a visualization technique called 't-SNE' (Maaten and Hinton, 2008). Generally, appropriate control parameters lead to high Q value, thus the agents tend to choose these parameters. As expected, the t-SNE algorithm tends to map the states with similar states closely. However, there are also some instances that the embedding is generated in terms of the Q values rather than the states. The reason is that neural networks are able to learn abstract features from the high-dimensional input. This conclusion is same as previous studies (Mnih et al., 2015).

### 3.2. Optimization under different scenarios

Fig. 6 demonstrates the influent and optimized control parameters vary from day 20 to day 30. Generally, with a large inflow rate, the concentrations of pollutants decrease because of the dilution process. In addition, the concentrations and inflow rate have significant periodicity with the daily schedule.

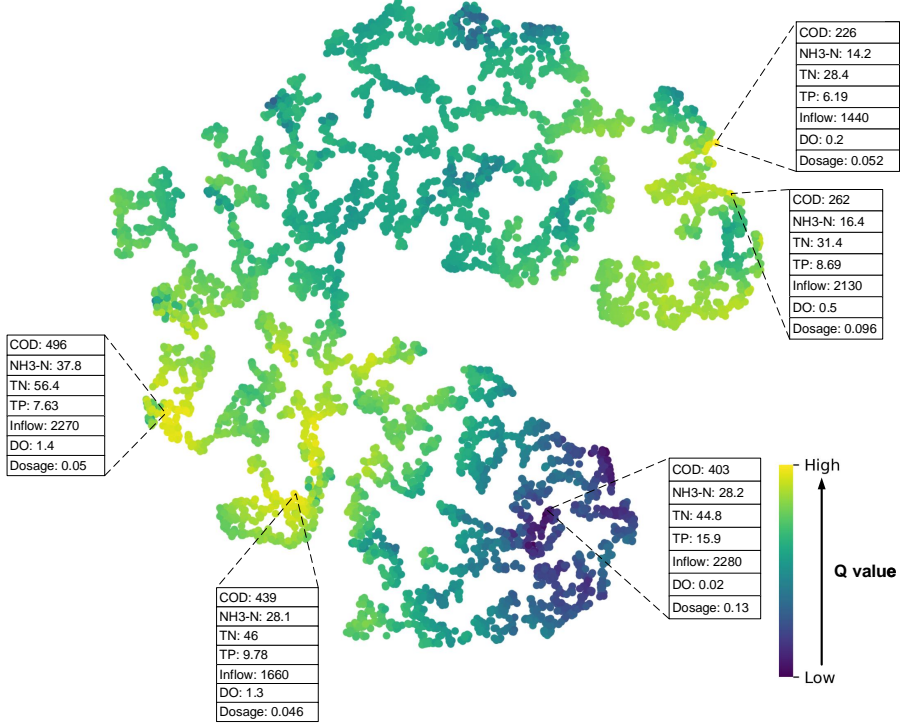


Figure 5: Two-dimensional t-SNE embedding of the input states.

Under most scenarios, the optimized DO and dosage maintain within a certain range due to the time dependence of biological system (Sniders and Laizans, 2011), if the control parameters change dramatically, the microbial community needs time to adapt or recovery from the shock. The mean DO values under LCA-IA, LCA-IB, cost and LCA-SW scenarios are 1.8, 1.4, 0.7 and 2.1  $mg/L$  (changed +20%, -6.7%, -53% and +40% compared to the baseline), respectively. The mean values of dosage are 0.084, 0.076, 0.080 and 0.255  $kg/m^3-ww$  (changed -32.8%, -39.2%, -36% and +104% compared to the baseline). We find that higher DO values but lower dosage are chosen by the agents to further optimize configuration, as the optimization is implemented under LCA-IA scenario. When the optimization only needs to meet Grade I-B standard, both DO and dosage are reduced significantly. When the energy, EP and GHG are not taken into account, cost scenario decreases DO to the most while ensures the effluent quality. As for LCA-SW, the dosage set-points show an obvious increase and fluctuation since the discharge standard of TP changes from 0.5 to 0.3  $mg/L$ .

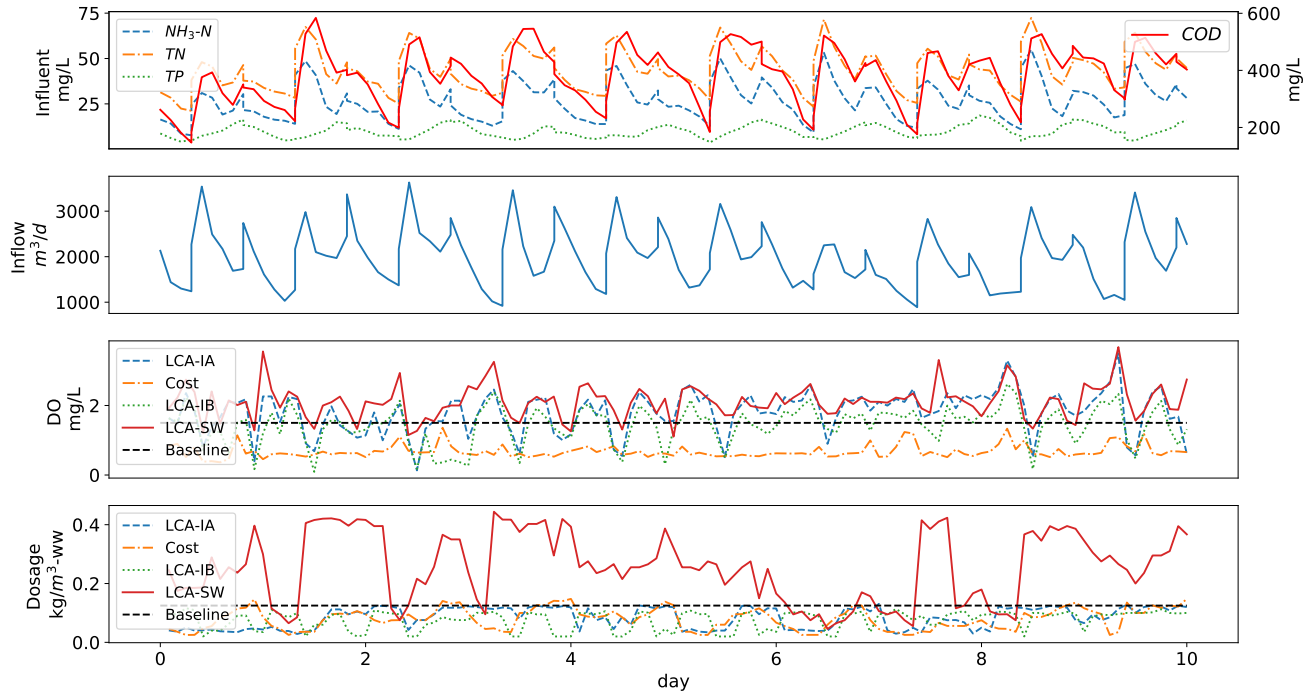


Figure 6: Influent and optimized control parameters with time.

Fig. 7 presents the impacts under five scenarios along with time. The baseline has a mediocre overall performance, but steady DO and dosage set-points provide a stable environment with low variance that is beneficial to the growth of microbial community. The Chinese government requires all WWTPs constructed after 2006 meeting the Grade I-A standard, hence Grade I-A standard is considered under most scenarios (Ministry, 2016). Compared to the baseline, the agents optimize the system from a comprehensive perspective under LCA-IA scenario. Specifically, DO is increased and dosage is decreased. As a result, the cost and energy consumption change from 0.432 to 0.402  $CNY/m^3\text{-}ww$  and 0.262 to 0.245  $kWh/m^3\text{-}ww$ , respectively. The DO and dosage are optimized by maintaining the effluent quality of ammonia (from 2.12 to 2.15  $mg/L$ ) and phosphorus (from 0.37 to 0.4  $mg/L$ ). In addition, the GHG emissions through biological processes under LCA-IA and baseline scenarios are nearly equal, and optimal parameters further lower the GHG emissions (from 1.998 to 1.966  $kgCO_2\text{-}eq/m^3\text{-}ww$ ) owing to the reduction of DO and dosage.

If the optimization is based on cost, the agents reduce both DO and dosage to decrease

energy consumption and cost. As shown in Fig. 6, cost scenario owns lowest DO rate. The cost under this scenario is only  $0.228 \text{ CNY}/m^3\text{-ww}$ . Nevertheless, the reduction in cost results in the decrease of contaminant removal efficiency, thus the eutrophication potential rises from 0.0032 to  $0.0036 \text{ kgPO}_4\text{-eq}/m^3\text{-ww}$ .

Apart from Grade I-A, Grade I-B and quasi standards IV for surface water are also taken into account. The results indicate that if the discharge standard is relaxed to Grade I-B, both energy consumption and cost are reduced with the sacrifice of effluent quality (change to  $0.0038 \text{ kgPO}_4\text{-eq}/m^3\text{-ww}$ ) as shown in Fig. 7. The optimization under LCA-SW scenario is implemented without retrofitting of the WWTP, i.e. using the same water treatment processes and technologies. Therefore, a large amount of extra DO and dosage are required to satisfy the stricter standard, and the improvement of effluent quality renders impact transfer or leakage. Compared to baseline scenario, the energy consumption, cost and GHG emissions under LCA-SW are  $0.337 \text{ kWh}/m^3\text{-ww}$ ,  $0.627 \text{ CNY}/m^3\text{-ww}$  and  $2.115 \text{ kgCO}_2\text{-eq}/m^3\text{-ww}$ , respectively. Besides, extra requirements are harmful to the system condition since the high variation. As a result, although the discharge pollutants reaches to  $0.0028 \text{ kgPO}_4\text{-eq}/m^3\text{-ww}$ , the updating of treatment technologies is more recommended when strict standard is required.

Table 3 lists the cumulative environmental variations within 10 days compared to the baseline. LCA-IA saves  $340 \text{ kWh}$ ,  $606 \text{ CNY}$  and  $636 \text{ kgCO}_2\text{-eq}$  during the 10-day simulation, while cost scenario spares  $678 \text{ kWh}$ ,  $894 \text{ CNY}$  and  $476 \text{ kgCO}_2\text{-eq}$ . Therefore, the LCA-IA and cost scenarios have comparable overall performance because cost scenario has higher eutrophication potential but saves more in other indicators, which means traditional cost-oriented optimization (Yamanaka et al., 2017) is effective to some extent. Similarly, a relaxed standard can also lead to satisfactory comprehensive results. As a result, the stakeholders should choose strategies according to the economic and ecological conditions. Last, LCA-SW scenario affords extra  $1486 \text{ kWh}$  energy consumption,  $3892 \text{ CNY}$  cost and  $2352 \text{ kgCO}_2\text{-eq}$  GHG emissions within 10 days, i.e. causing large negative environmental and economic impacts.

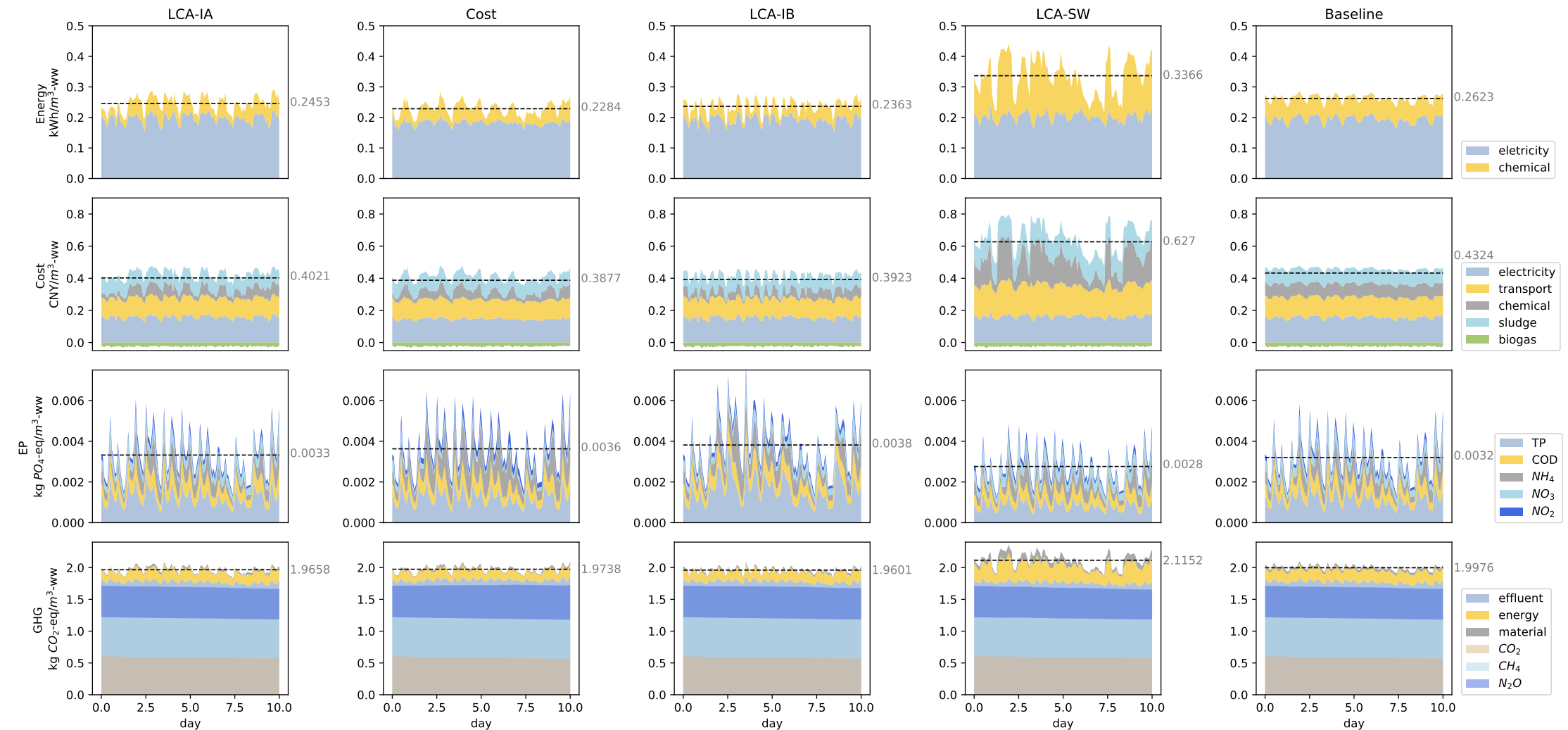


Figure 7: LCA and cost impacts under five scenarios.

Table 3: Cumulative environmental impacts within 10 days compared to baseline

Scenario	Energy (kWh)	Cost (CNY)	EP (kgPO <sub>4</sub> -eq)	GHG (kgCO <sub>2</sub> -eq)
LCA-IA	-340	-606	+2	-636
Cost	-678	-894	+8	-476
LCA-IB	-520	-802	+12	-750
LCA-SW	+1486	+3892	-8	+2352

### 3.3. Component analysis

Among the five scenarios (Fig. 8), around 50% of the energy consumption is caused by aeration process and pumps, which is consistent with previous studies (Panepinto et al., 2016). The fixed electricity takes up  $\sim$ 30% of the total energy consumption. Generally, the chemical consumption accounts for 14-20% of the total energy consumption. Therefore, the reduction of aeration rate and dosage is the most important and manipulable step to achieve energy saving.

From cost perspective, electricity and transport cost account for the majority of the expenditure. In addition, the produced sludge not only influences the transport cost, but also determines land-filling cost. According to the results, the cost resulting from sludge treatment accounts for about 20% of the total transport cost. Moreover, the cost of land-filling is also non-negligible. In China, land-filling is the cheapest method for sludge disposal, other methods such as incineration and building materials normally spend several times more money (Yang et al., 2015). Hence, the sludge reduction technologies (Foladori et al., 2010) and economical disposal approaches (Gherghel et al., 2019) have received great attention recently.

Phosphate is the main contributor of eutrophication potential, thus, how to remove or recover phosphorus from wastewater efficiently and economically is another valuable topic (Wilfert et al., 2015). Besides, ammonia is another important factor with high eutrophication potential, thus the strict standards normally require low TP and ammonia concentrations. Under five scenarios, around 50% phosphorus is removed through biological process. Low DO

set-points such as cost scenario enhance the biological phosphorus removal ( $\sim 55\%$ ) since the reduction of heterotrophic bacteria (XBH) activity. As a cost effective method, enhanced biological phosphorus removal is worth considering (Bunce et al., 2018). The analysis of microbial community shows that the concentrations of four microorganisms: heterotrophic bacteria (XBH), ammonia oxidizing bacteria (AOB), nitrifying bacteria (NOB), polyphosphate accumulating bacteria (PAO) are identical under five scenarios. However, aluminum salt can inhibit biological phosphorus release and uptake processes significantly, as well as inhibit AOB dominantly (Liu et al., 2011). In the simulation, the inhibition process is not considered.

As for the GHG emission, the simulation results show that GHG emitted from biological processes occupies over 80 % of the total GHG emissions. As the release of  $\text{CO}_2$  is inevitable, and most  $\text{CH}_4$  is collected,  $\text{N}_2\text{O}$  is of great importance to the global warming.  $\text{N}_2\text{O}$  is produced during both nitrification and denitrification processes (Kampschreur et al., 2009), and the global warming potential of  $\text{N}_2\text{O}$  is 298 times higher than  $\text{CO}_2$ . Kampschreur et al. (2009) concluded that low DO concentration in the nitrification stage, high nitrite concentrations, and low COD/N ratio in the denitrification stage are three main operational parameters leading to  $\text{N}_2\text{O}$  emissions. Hence, how to reduce  $\text{N}_2\text{O}$  effectively and economically is another research topic.

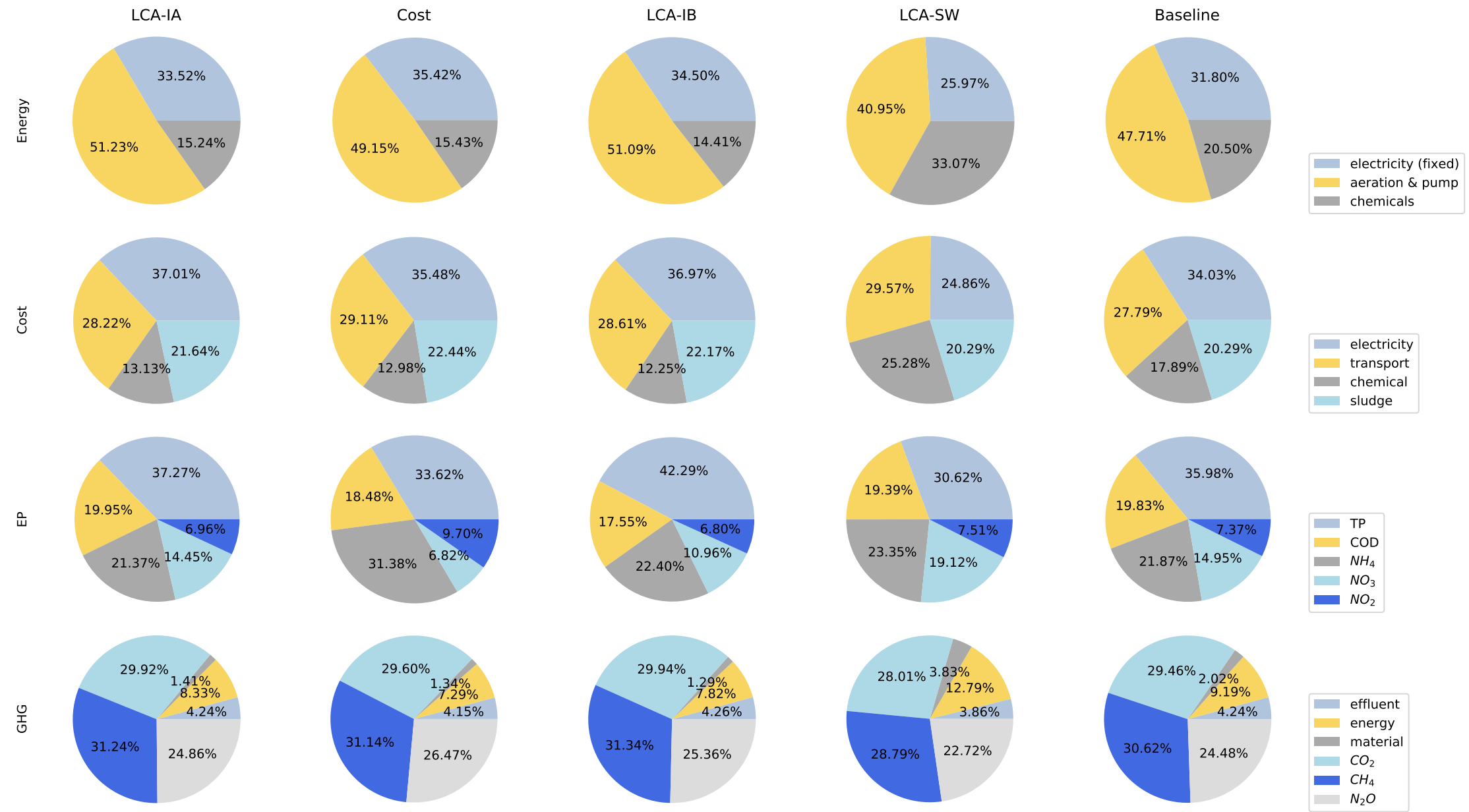


Figure 8: Component proportion of five scenarios.

### 3.4. The selection of control strategies

As discussed above, different optimization orientations have different environmental impacts. Cost-oriented and LCA-oriented control strategies have comparable performance in this study, however, LCA-based strategies have high extendability when other environmental indicators are considered.

Besides, if the recipient stream is sensitive to pollutants, the implementation of strict standards is imperative. Nevertheless, similar to the previous study from [Sweetapple et al. \(2014\)](#), LCA-SW strategy is a case that effluent quality is considered as the dominant factor of optimization, but causes severe impact transfer. Conversely, technology-driven upgrading consumes materials and energy during construction, but may cut down side effects during operation. Here, scheme comparisons are recommended for reasonable retrofitting. On the other hand, if the environmental carrying capacity ([Liu and Borthwick, 2011](#)) in the target area is high, using relaxed discharge standards (such as Class I-B) is also an alternative.

As the most common strategy, default baseline strategies maintain control parameters at constant levels by a simple closed-loop configuration consisting of PI controllers ([Nopens et al., 2010](#)), these strategies have acceptable performance, and provide stable environment for the microbial community. As for dynamic control strategies, they require real-time influent and effluent quality. There are two methods to acquire real-time data. The first method is to install advanced sensors ([Campisano et al., 2013](#)) requiring high expenditure for purchasing and operating. The second one is to predict data using machine learning algorithms ([Zhou et al., 2019; Wang et al., 2019](#)), such algorithms are trivial to achieve, but require numerous data and suffer from high uncertainty. In a summary, dynamic control strategies are promising but still challenging at present.

### 3.5. Limitation and future work

Multi-objective reinforcement learning is still under initiative stage ([Liu et al., 2014](#)). In this work, a scalar reward function rather than the Pareto strategy is used. Scalar scheme is easy to understand and optimize, but cannot obtain Pareto front, which causes difficulties to strategy generation. In addition, same values of a scalar reward may indicate multiple

action pairs which also brings confusion. Thus, other algorithms using Pareto framework (Van Moffaert and Nowé, 2014) can be applied in future work. Besides, RL algorithm is sensitive to reward function, hence the reward engineering can impact performance significantly (Dewey, 2014). This study is a trial of LCA based reward engineering and heuristic method such as the extra constraint is imperative to avoid unrealistic results. In addition, the weights and factors impact optimization results dramatically. The determination of these parameters is according to the rule-of-thumb in this study. To sum up, performance of non-weighted approaches should be further investigated in future work, and an efficient reward engineering method for WWTP evaluation is also needed to be explored.

Most algorithms of RL are model-free. As data-driven algorithms, they normally require a large number of samples from the real world or models. Hence the accuracy of model determines the results. In addition, the dynamic GHG model is still under research stage (Corominas et al., 2012), and some bias is introduced by models. For example, GHG emissions from clarifiers are ignored in our GHG model; the inhibition of microbial community is not considered as mentioned above. Furthermore, complicated mechanism models require high computational power, which also increase the training time (Corominas et al., 2012). Considering that training models requires plenty of time, the size of replay buffer is selected as 1000 during learning stage. Besides, DRL introduces neural networks as feature representatives, therefore, there are plenty of hyperparameters that create difficulties when acquiring good performance. When the algorithm is deployed in field, the data size is usually limited. In short, the WWTP in this study lacks of huge amounts of in-filed operational data for validation, in the future, this novel algorithm should be implemented in field to verify the performance.

Last, the system boundary of LCA is limited to the WWTP and merely three mid-point indicators are chosen because these indicators represents the major concerns in WWTPs and the data of these indicators are easy to acquire or calculate by models. A complete system boundary and ample indicators lead to complete results, but also require lots of data and introduce uncertainty. Thus, the building of data centers of WWTPs is necessary in the future.

## 4. Conclusion

This study applied multi-agent deep reinforcement learning to optimize DO and dosage simultaneously. An LCA-based reward function is designed for sustainability optimization. The results show that:

- (1) The novel MADDPG algorithm learns abstracts features from high-dimensional states, and influents with proper control variables have high Q values;
- (2) Optimization based on LCA has lower environmental impacts compared to baseline scenario. The cost-oriented control strategy owns comparable performance to the LCA-driven strategy, but with less extendability;
- (3) Environmental impacts under different discharge standards are analysed. The stakeholders should formulate standards in terms of environmental carrying capability. It is worth mentioning that the retrofitting of WWTPs based on resources should be implemented with the consideration of impact transfer;
- (4) The major contributors of each indicators are identified for future study and improvement. Specifically, the reduction of aeration and chemical dosage lower both energy and cost significantly, while sludge disposal is another vital point for cost reduction. Enhanced phosphorus and ammonia removal further decreases the eutrophication potential. Besides, how to reduce nitrous oxide economically and effectively is another valuable topic;
- (5) Last, we discuss that novel dynamic control strategies require advanced sensors or a large amount of data, so the selection of control strategies should also consider economic and ecological conditions.

## Acknowledgements

We gratefully acknowledge the financial support by the Natural Science foundation of China(No.52000054), the NSFC-EU Environmental Biotechnology joint program (No.31861133001) and Shenzhen Science and Technology Program (Grant No. KQTD20190929172630447).

## References

D. Rosso, M. K. Stenstrom, The carbon-sequestration potential of municipal wastewater treatment, *Chemosphere* 70 (2008) 1468–1475.

T. Yang, W. Qiu, Y. Ma, M. Chadli, L. Zhang, Fuzzy model-based predictive control of dissolved oxygen in activated sludge processes, *Neurocomputing* 136 (2014) 88–95.

L. Åmand, G. Olsson, B. Carlsson, Aeration control—a review, *Water Science and Technology* 67 (2013) 2374–2398.

C. M. Castro-Barros, M. Daelman, K. Mampaey, M. Van Loosdrecht, E. Volcke, Effect of aeration regime on n<sub>2</sub>o emission from partial nitritation-anammox in a full-scale granular sludge reactor, *water research* 68 (2015) 793–803.

B. Holenda, E. Domokos, A. Redey, J. Fazakas, Dissolved oxygen control of the activated sludge wastewater treatment process using model predictive control, *Computers & Chemical Engineering* 32 (2008) 1270–1278.

M. Grochowski, T. A. Rutkowski, Supervised model predictive control of wastewater treatment plant, in: 2016 21st International Conference on Methods and Models in Automation and Robotics (MMAR), IEEE, pp. 613–618.

D. Silver, A. Huang, C. J. Maddison, A. Guez, L. Sifre, G. Van Den Driessche, J. Schrittwieser, I. Antonoglou, V. Panneershelvam, M. Lanctot, et al., Mastering the game of go with deep neural networks and tree search, *nature* 529 (2016) 484.

L. P. Kaelbling, M. L. Littman, A. W. Moore, Reinforcement learning: A survey, *Journal of artificial intelligence research* 4 (1996) 237–285.

F. Hernández-del Olmo, F. H. Llanes, E. Gaudioso, An emergent approach for the control of wastewater treatment plants by means of reinforcement learning techniques, *Expert Systems with Applications* 39 (2012) 2355–2360.

S. Syafie, F. Tadeo, E. Martinez, T. Alvarez, Model-free control based on reinforcement learning for a wastewater treatment problem, *Applied Soft Computing* 11 (2011) 73–82.

C. J. Watkins, P. Dayan, Q-learning, *Machine learning* 8 (1992) 279–292.

J. Pang, S. Yang, L. He, Y. Chen, N. Ren, Intelligent control/operational strategies in wwtps through an integrated q-learning algorithm with asm2d-guided reward, *Water* 11 (2019a) 927.

J.-W. Pang, S.-S. Yang, L. He, Y.-D. Chen, G.-L. Cao, L. Zhao, X.-Y. Wang, N.-Q. Ren, An influent responsive control strategy with machine learning: Q-learning based optimization method for a biological phosphorus removal system, *Chemosphere* 234 (2019b) 893–901.

P. Petsagkourakis, I. O. Sandoval, E. Bradford, D. Zhang, E. A. del Rio-Chanona, Reinforcement learning for batch bioprocess optimization, *Computers & Chemical Engineering* 133 (2020) 106649.

J. Filipe, R. J. Bessa, M. Reis, R. Alves, P. Póvoa, Data-driven predictive energy optimization in a wastewater pumping station, *Applied Energy* 252 (2019) 113423.

A. B. B. de Faria, A. Ahmadi, L. Tiruta-Barna, M. Spérando, Feasibility of rigorous multi-objective optimization of wastewater management and treatment plants, *Chemical Engineering Research and Design* 115 (2016) 394–406.

Y. Li, Y. Huang, Q. Ye, W. Zhang, F. Meng, S. Zhang, Multi-objective optimization integrated with life cycle assessment for rainwater harvesting systems, *Journal of hydrology* 558 (2018) 659–666.

A. Ahmadi, L. Tiruta-Barna, A process modelling-life cycle assessment-multiobjective optimization tool for the eco-design of conventional treatment processes of potable water, *Journal of Cleaner Production* 100 (2015) 116–125.

S. Sötemann, P. Van Rensburg, N. Ristow, M. Wentzel, R. Loewenthal, G. Ekama, Integrated chemical/physical and biological processes modeling part 2-anaerobic digestion of sewage sludges, *Water Sa* 31 (2005) 545–568.

P. Van Rensburg, E. Musvoto, M. Wentzel, G. Ekama, Modelling multiple mineral precipitation in anaerobic digester liquor, *Water Research* 37 (2003) 3087–3097.

K. V. Gernaey, X. Flores-Alsina, C. Rosen, L. Benedetti, U. Jeppsson, Dynamic influent pollutant disturbance scenario generation using a phenomenological modelling approach, *Environmental Modelling & Software* 26 (2011) 1255–1267.

X. Flores-Alsina, K. V. Gernaey, U. Jeppsson, Benchmarking biological nutrient removal in wastewater treatment plants: influence of mathematical model assumptions, *Water Science and Technology* 65 (2012) 1496–1505.

T. P. Lillicrap, J. J. Hunt, A. Pritzel, N. Heess, T. Erez, Y. Tassa, D. Silver, D. Wierstra, Continuous control with deep reinforcement learning, *arXiv preprint arXiv:1509.02971* (2015).

V. Mnih, K. Kavukcuoglu, D. Silver, A. A. Rusu, J. Veness, M. G. Bellemare, A. Graves, M. Riedmiller, A. K. Fidjeland, G. Ostrovski, et al., Human-level control through deep reinforcement learning, *Nature* 518 (2015) 529–533.

R. Lowe, Y. I. Wu, A. Tamar, J. Harb, O. P. Abbeel, I. Mordatch, Multi-agent actor-critic for mixed cooperative-competitive environments, in: *Advances in neural information processing systems*, pp. 6379–6390.

D. Silver, G. Lever, N. Heess, T. Degris, D. Wierstra, M. Riedmiller, Deterministic policy gradient algorithms.

D. P. Kingma, J. Ba, Adam: A method for stochastic optimization, *arXiv preprint arXiv:1412.6980* (2014).

N. Ketkar, Introduction to pytorch, in: *Deep learning with python*, Springer, 2017, pp. 195–208.

G. Brockman, V. Cheung, L. Pettersson, J. Schneider, J. Schulman, J. Tang, W. Zaremba, Openai gym,

arXiv preprint arXiv:1606.01540 (2016).

Alibaba, Alibaba, <https://www.1688.com>, 2020.

G. Yang, G. Zhang, H. Wang, Current state of sludge production, management, treatment and disposal in china, *Water research* 78 (2015) 60–73.

X. Jiang, S. G. Sommer, K. V. Christensen, A review of the biogas industry in china, *Energy Policy* 39 (2011) 6073–6081.

S. Longo, M. Mauricio-Iglesias, A. Soares, P. Campo, F. Fatone, A. L. Eusebi, E. Akkersdijk, L. Stefani, A. Hospido, Enerwater—a standard method for assessing and improving the energy efficiency of wastewater treatment plants, *Applied Energy* 242 (2019) 897–910.

CML, Cml 2001 impact assessment method, 2002.

R. Goel, A. Blackbourn, Z. Khalil, M. Yendt, H. Monteith, Implementation of carbon footprint model in a dynamic process simulator, *Proceedings of the Water Environment Federation* 2012 (2012) 2413–2426.

S. Eggleston, L. Buendia, K. Miwa, T. Ngara, K. Tanabe, 2006 IPCC guidelines for national greenhouse gas inventories, volume 5, Institute for Global Environmental Strategies Hayama, Japan, 2006.

H. Wang, Y. Yang, A. A. Keller, X. Li, S. Feng, Y.-n. Dong, F. Li, Comparative analysis of energy intensity and carbon emissions in wastewater treatment in usa, germany, china and south africa, *Applied Energy* 184 (2016) 873–881.

V. Parraviciniak, K. Svardala, J. Krampea, Greenhouse gas emissions from wastewater treatment plants, *Energy Procedia* 97 (2016) 246–253.

D. de Haas, J. Foley, K. Barr, Greenhouse gas inventories from wwtts—the trade-off with nutrient removal, *Proceedings of the Water Environment Federation* 2008 (2008) 264–285.

Z. Zhang, B. Wang, Research on the life-cycle co2 emission of china's construction sector, *Energy and Buildings* 112 (2016) 244–255.

M. Pizzol, A. Laurent, S. Sala, B. Weidema, F. Verones, C. Koffler, Normalisation and weighting in life cycle assessment: quo vadis?, *The International Journal of Life Cycle Assessment* 22 (2017) 853–866.

X. Wang, P. L. McCarty, J. Liu, N.-Q. Ren, D.-J. Lee, H.-Q. Yu, Y. Qian, J. Qu, Probabilistic evaluation of integrating resource recovery into wastewater treatment to improve environmental sustainability, *Proceedings of the National Academy of Sciences* 112 (2015) 1630–1635.

o. E. P. Ministry, Action plan for water pollution prevention and control, China (2014).

Q. Zhang, W. Yang, H. Ngo, W. Guo, P. Jin, M. Dzakpasu, S. Yang, Q. Wang, X. Wang, D. Ao, Current status of urban wastewater treatment plants in china, *Environment international* 92 (2016) 11–22.

L. v. d. Maaten, G. Hinton, Visualizing data using t-sne, *Journal of machine learning research* 9 (2008) 2579–2605.

A. Sniders, A. Laizans, Adaptive model of wastewater aeration tank, *Environmental and Climate Technolo-*

gies 6 (2011) 112–117.

o. E. P. o. C. Ministry, Discharge standard of pollutants for urban wastewater treatment plant, 2016.

O. Yamanaka, Y. Onishi, R. Namba, T. Obara, Y. Hiraoka, A total cost minimization control for wastewater treatment process by using extremum seeking control, *Water Practice & Technology* 12 (2017) 751–760.

D. Panepinto, S. Fiore, M. Zappone, G. Genon, L. Meucci, Evaluation of the energy efficiency of a large wastewater treatment plant in italy, *Applied Energy* 161 (2016) 404–411.

P. Foladori, G. Andreottola, G. Ziglio, Sludge reduction technologies in wastewater treatment plants, IWA publishing, 2010.

A. Gherghel, C. Teodosiu, S. De Gisi, A review on wastewater sludge valorisation and its challenges in the context of circular economy, *Journal of cleaner production* 228 (2019) 244–263.

P. Wilfert, P. S. Kumar, L. Korving, G.-J. Witkamp, M. C. van Loosdrecht, The relevance of phosphorus and iron chemistry to the recovery of phosphorus from wastewater: a review, *Environmental science & technology* 49 (2015) 9400–9414.

J. T. Bunce, E. Ndam, I. D. Ofiteru, A. Moore, D. W. Graham, A review of phosphorus removal technologies and their applicability to small-scale domestic wastewater treatment systems, *Frontiers in Environmental Science* 6 (2018) 8.

Y. Liu, H. Shi, W. Li, Y. Hou, M. He, Inhibition of chemical dose in biological phosphorus and nitrogen removal in simultaneous chemical precipitation for phosphorus removal, *Bioresource technology* 102 (2011) 4008–4012.

M. J. Kampschreur, H. Temmink, R. Kleerebezem, M. S. Jetten, M. C. van Loosdrecht, Nitrous oxide emission during wastewater treatment, *Water research* 43 (2009) 4093–4103.

C. Sweetapple, G. Fu, D. Butler, Multi-objective optimisation of wastewater treatment plant control to reduce greenhouse gas emissions, *Water Research* 55 (2014) 52–62.

R. Liu, A. G. Borthwick, Measurement and assessment of carrying capacity of the environment in ningbo, china, *Journal of environmental management* 92 (2011) 2047–2053.

I. Nopens, L. Benedetti, U. Jeppsson, M.-N. Pons, J. Alex, J. B. Copp, K. V. Gernaey, C. Rosen, J.-P. Steyer, P. A. Vanrolleghem, Benchmark simulation model no 2: finalisation of plant layout and default control strategy, *Water Science and Technology* 62 (2010) 1967–1974.

A. Campisano, J. Cabot Ple, D. Muschalla, M. Pleau, P. A. Vanrolleghem, Potential and limitations of modern equipment for real time control of urban wastewater systems, *Urban Water Journal* 10 (2013) 300–311.

P. Zhou, Z. Li, S. Snowling, B. W. Baetz, D. Na, G. Boyd, A random forest model for inflow prediction at wastewater treatment plants, *Stochastic Environmental Research and Risk Assessment* 33 (2019) 1781–1792.

Z. Wang, Y. Man, Y. Hu, J. Li, M. Hong, P. Cui, A deep learning based dynamic cod prediction model for urban sewage, *Environmental Science: Water Research & Technology* 5 (2019) 2210–2218.

C. Liu, X. Xu, D. Hu, Multiobjective reinforcement learning: A comprehensive overview, *IEEE Transactions on Systems, Man, and Cybernetics: Systems* 45 (2014) 385–398.

K. Van Moffaert, A. Nowé, Multi-objective reinforcement learning using sets of pareto dominating policies, *The Journal of Machine Learning Research* 15 (2014) 3483–3512.

D. Dewey, Reinforcement learning and the reward engineering principle, in: 2014 AAAI Spring Symposium Series.

L. Corominas, X. Flores-Alsina, L. Snip, P. A. Vanrolleghem, Comparison of different modeling approaches to better evaluate greenhouse gas emissions from whole wastewater treatment plants, *Biotechnology and Bioengineering* 109 (2012) 2854–2863.